Int. J. Electrochem. Sci., 15 **(2020)** 5741 – 5757, doi: 10.20964/2020.06.70

International Journal of
ELECTROCHEMICAL
SCIENCE
www.electrochemsci.org

Study on the Electrodeposition of Chromium from Cr(III) Solution in the Presence of Oxalate and Acetate Anions

Dennys Fernández Conde[*], *German Orozco Gamboa, Julieta Torres González.*

Centro de Investigación y Desarrollo Tecnológico en Electroquímica.
Parque Tecnológico Qro. Sanfandila, P.O. Box 76703, Pedro Escobedo, Querétaro, México.
[*]E-mail: dfernandez@cideteq.mx

Received: 27 November 2019 / *Accepted:* 2 April 2020 / *Published:* 10 May 2020

A Hull cell was used to evaluate a chromium(III) plating bath based on the combination of oxalate and acetate anions. The bath contains chromium(III) sulfate, ammonium oxalate, sodium acetate, boric acid, potassium sulfate, sodium sulfate and sodium dodecyl sulfate (SDS). The working pH was 3.5, and all species were protonated. The chromium(III) plating bath had a faradaic efficiency of 37%, high covering power at 8.2 cm, low deposition potential of 7.3 V, and a deposition rate of 0.4 μm/min. Chromium coatings were obtained at a current density (30A/dm^2). This chromium(III) plating bath is competitive considering the state of the art of the electrodeposition of Cr(III). SDS was used as a surfactant to prevent the formation of polymeric oxides (olation reactions) by decreasing the number of nearby ions of Cr(III). Boric acid successfully maintained the pH as a buffer because after 2 h of the electrodeposition process, the pH values change only 0.2 units. The bath was analyzed after electrolysis to check the formation of Cr(VI) ions, and after 2 h of electrodeposition, this cation was not detected. The voltammetry results showed a very high noise with a potential of -0.8 V due to the abundant bubbles that formed and suggest a reduction in a step from Cr(III) to Cr(0). In the literature, the use of oxalate anions is explained by the reaction of exchange of ligands between these anions and the water of the first solvation sphere of Cr(III). In our study, it is postulated that electrostatic interactions of ion-ions and ion-solvents should be very present, and that oxalate and acetate anions are very likely to be in the second sphere of solvation and not in the first as other authors propose. The water molecules in the first solvation sphere are very stable and difficult to replace because they are exposed to two opposite electrostatic forces at their ends.

Keywords: chromium(III) plating bath, solvation sphere, ligands, chromium electrodeposits, hull cell.

1. INTRODUCTION

The chromium(III) plating baths have received a lot of attention in the 21st century because the toxicity of Cr(III) is much lower than that of Cr(VI). In 1933, Kasper[1] reviewed the literature on chromium(III) plating baths published up to that date and concluded that these baths have poor

performance because they produce poor deposits and require high current densities. In 2014, Protsenko[2] reviewed several baths and proposed several parameters to be taken into account for a comparison between trivalent and hexavalent chromium baths. This group emphasized the environmental safety and shelf life of these chromium(III) plating baths and concluded that some may have promising performance[3-11]; however, more efforts are needed to obtain coatings with a high quality hardness.

In 1932, Britton and Westcott[12] were the pioneers in the use of additives in chromium(III) plating baths and observed that ammonium oxalate produced good chromium deposits with lower faradaic efficiency. Since then, some researchers have been trying to develop chromium(III) plating baths by adding oxalate anions[13-19], obtaining promising coatings regarding their corrosion resistance and mechanical strength. Gines[20] used acetate as an additive and $CrCl_3.6H_2O$ as a source of Cr(III) ions in the chromium bath with acceptable results. On the other hand, Protsenko[2] obtained a coating with good quality using chromium(III) sulfate. In the present study, the combination of acetate and oxalate ligands was studied as the main substances in the chromium(III) plating bath, in addition to chromium(III) sulfate as a source of Cr(III). It should be noted that the combination of these ligands in bath composition has not been explored, since several authors use other ligands such as formiate, glycine, etc.

Protsenko[2] makes it very clear that the formation of Cr(VI) in chromium(III) plating baths is a serious disadvantage due to the increased cost in the treatment of the generated wastewater. Several chromium(III) plating baths studies[2-12, 15, 19] show that the use of a Hull cell (electrochemical cell) is very useful for optimizing very important parameters such as current density, pH and time of electrodeposition, however, the composition of the bath is not reported after electrolysis; therefore, it is not possible to determine if these baths produce Cr(VI) ions. Based on this concern, the experimental baths were analyzed before and after electrolysis to detect possible Cr(VI) ions formation.

2. EXPERIMENTAL

The following analytical grade reagents were used for bath preparation: chromium(III) sulfate ($Cr_2(SO_4)_3{\cdot}6H_2O$, JT Baker USA), boric acid (H_3BO_3, JT Baker USA), sodium sulfate (Na_2SO_4, anhydrous, Karal USA), sodium acetate (CH_3COONa, anhydrous, JT Baker USA), hydrated ammonium oxalate ($(COONH_4)_2$, Meyer USA) and sodium dodecyl sulfate ($CH_3(CH_2)_{11}OSO_3Na$, JT Baker USA). The baths were prepared with water produced by an ELIX 70-Merck Millipore deionization system (conductivity = 18.2 MQ.cm). Reagents were added to the chromium(III) plating bath every 10 minutes. The first solutions contained few elements, and then more substances were added to understand their effect on the electrodeposition process. The final composition and concentration is listed in Table 1.

A PerkinElmer Lambda XLS UV-visible spectrophotometer was used to obtain the spectrum of each bath after preparation and the electrodeposition process. In this study, a Hull cell, McGean-Rohco brand Cleveland, Ohio, USA was used with stirring and temperature control. A 0-30V/0-10A adjustable DC power source BK-Precision 672 model TripleOut 0-32V/0-6A DC was used.

The cathode was a brass plate from the Kocour Company, and the anode was a glassy carbon plate.

Table 1. Reagents used in chromium(III) plating bath preparation.

Reagents	**Conc.(m/L)**	
Chromium Sulfate	0.3	Chromium source
Ammonium Oxalate	0.3	Additive
Sodium Acetate	0.21	Additive
Boric Acid	0.97	Buffer
Potassium Sulfate	0.3	Conductive salt
Sodium Sulfate	0.35	Conductive salt
Sodium Dodecyl Sulfate	$5.8x10^{-4}$	Surfactant

The electrode surfaces were cleaned with 10% H_2SO_4 for 2 minutes before the measurements. Chromium electrodeposition was performed by applying a current between the terminals of the 3A Hull cell for 10 minutes at room temperature. The pH and conductivity of the chromium(III) plating bath were monitored during the process with a pH meter, HANNA Instruments model HI 2550 pH/ORP and EC/TDS NaCl. Based on the German standard DIN50957, the current density at a certain position of the hull plate was calculated using equation (1).

$$i_L = I_{ap} * (a- (b * \log L) \quad \textbf{(1)}$$

where i_L is the current density calculated in A/dm^2 for a certain distance (L) on the hull plate in cm, (I_{ap}) is the current applied in amps. In addition, a and b are constant values of 5.10 and 5.24 cm, respectively, taken by R. O. Hull and Mc Intear.

Diagrams of the predominance of species are based on the mass balance (equation 2) and the α fraction of the species (equation (3). In the construction of the diagrams the acid dissociation constant and the stability constants were used of the Cr^{3+} complexes with the molecules of these acids. In each diagram, the values of the constant and the data source are indicated.

$$P_t = \left[H_3PO_4^0\right] + \left[H_2PO_4^-\right] + \left[HPO_4^{2-}\right] + \left[PO_4^{3-}\right] \quad \textbf{(2)}$$

$$\alpha_{H_xPO_4^{x-3}} = \frac{[H_xPO_4^{x-3}]}{P_t} \quad \textbf{(3)}$$

Electrochemical measurements (cyclic voltammetry) at room temperature of 23 ± 2 °C were carried out with the PARSTAT 2273 potentiostat / galvanostat model with a conventional three electrode configuration, using a reference electrode of mercury sulfate saturated (0.68 V vs NHE). The morphology and structure of the coatings were determined using Jeol 6510LV scanning electron microscopy (SEM) with a dispersive energy X-ray spectroscopy (EDS) probe.

The faradaic efficiency of the electrodeposition was calculated based on the equation below:

$$FE(\%)=\frac{n*N*F}{Q}x100 \quad \textbf{(4)}$$

where *N* is the amount of the electrodeposited chromium in the process in moles, (51.996 gmol-1); *F* is the faradaic constant, 96485 C/mol; n is the number of electrons transferred in the faradaic process (n=3); *Q* is the total charge passed through the Hull cell.

3. RESULTS AND DISCUSSION

In the Hull cell, during the electrodeposition process the temperature reached values between 45-50 °C over time, similar to other studies in this cell[2-12, 15, 19]. The images of the plates obtained using the Hull cell show that in the bath without additives no chromium coating was obtained, only a deposit that appeared to be burned (Fig. 1a). In the bath with the acetate ions a chromium coating was obtained, but of very poor quality (Fig. 1b), the oxalate ion bath (Fig. 1c) shows a varied coating in terms of color, an opaque and semi-gloss white color appearing along the tank. Finally, the bath with the two additives combined produced a chromium coating with good quality and a glossy surface (Fig. 1d).

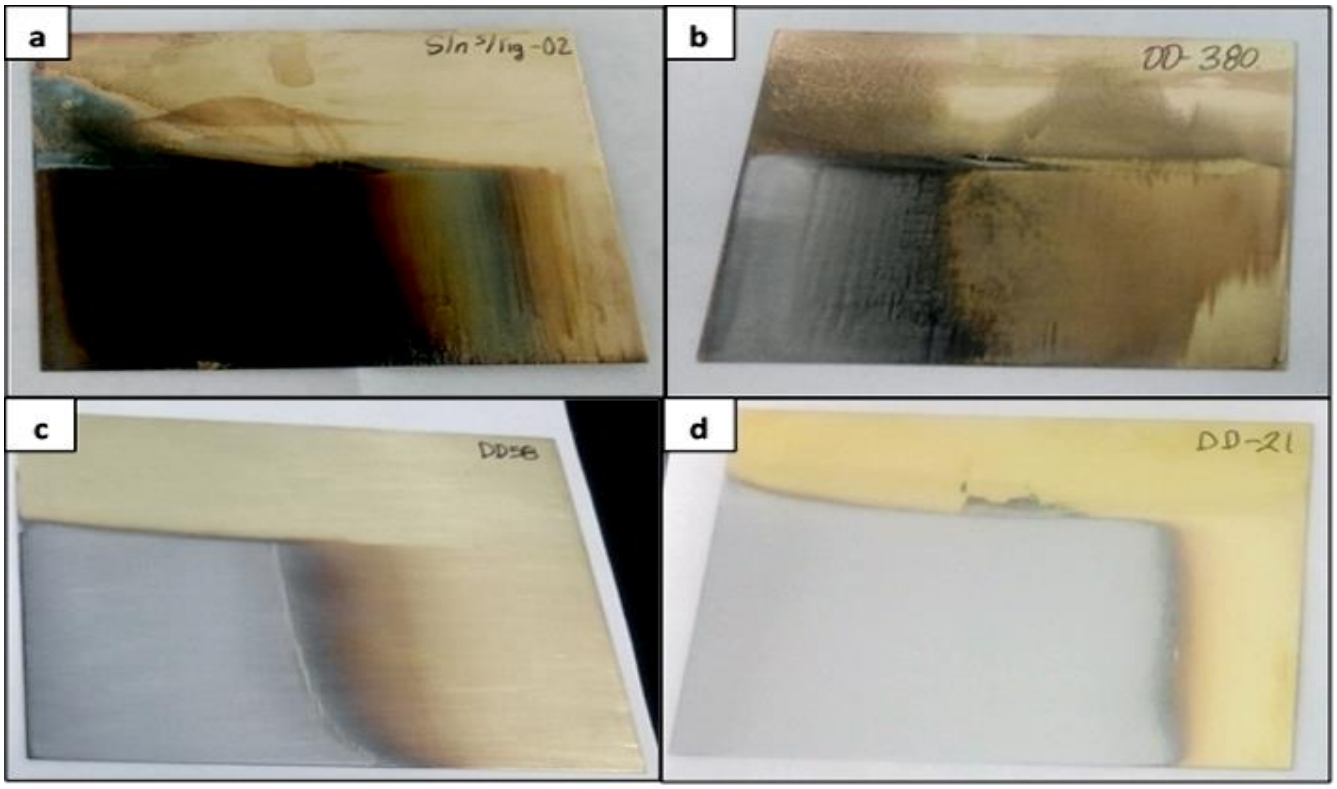

Figure 1. Hull plates obtained in chromium(III) plating baths after 10 min. a) without additives, the chromium source, the buffer, the two conductive salts, and the surfactant (see Table 1); b) with the acetate additive, the chromium source, buffer, two conductive salts and surfactant (Table 1); c) with the oxalate additive, the chromium source, buffer, two conductive salts and surfactant (Table 1); d) with both additives, the chromium source, buffer, two conductive salts and surfactant (Table 1).

The quantitative experimental data in Fig. 2 indicate a better performance in the baths where the 2 additives were combined. The burnt coatings of the bath without additive exhibited a very low covering power (1.2 cm in Fig. 2a), while the coatings obtained from the baths with the acetate or oxalate ions separately show a covering power of 3.2 cm (Fig. 2b) and 4.0 cm (Fig. 2c), respectively. These values are similar to the values reported by Protsenko[2] and Danilov[21] for a chromium(III) plating bath at 35 °C (see Table 2).

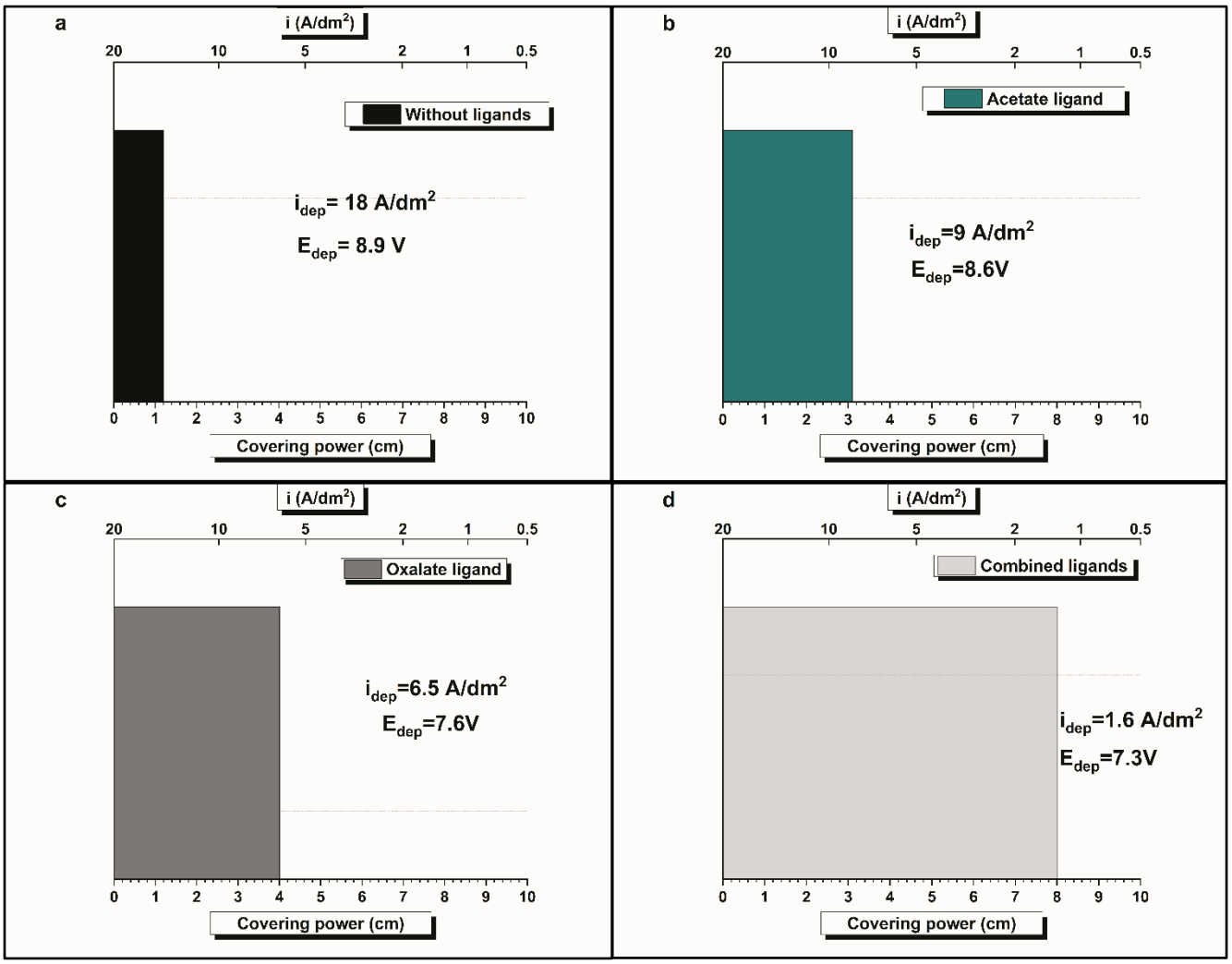

Figure 2. Comparison of the covering power of a) a bath without additives, only the source of chromium; b) a bath with acetate ions; c) a bath with oxalate ions; and d) a bath with two additives (oxalate and acetate). In addition, the obtained E_{dep} and i_{dep} values are shown.

On the other hand, in the bath with the combined oxalate and acetate ions, a covering power of 8.2 cm was obtained (Fig. 2d), which is similar to the values observed in a 6.0 cm commercial hexavalent chromium bath (Table 2). When no additive is present in the bath, the deposition potential and current will have high values (Fig. 2a). When in the bath there is presence of any of these ions (either oxalate or acetate) the potential and electrodeposition current continues with high values (Fig. 2b-2c). On the other hand, with the combination of both additives in the bath, both the deposition potential and the current

decrease, reaching values of 7.3 V and 1.6A/dm^2 respectively, obtaining, as shown in Fig. 1d, a chromium coating with a shiny surface.

In recent years, several improvements in chromium(III) plating baths have been reported in the literature[3-11]. For example, Protsenko[6] observed a 50% increase in bath faradaic efficiency when working at a current density of 20 A/dm^2, at a pH value of 1.9 and at an electrodeposition temperature of 35 °C. Very high data important to take into account in the baths are, the distance between the electrodes (gap) and the resistance of the solution, but unfortunately these are not reported in the studies. Table 2 shows a comparison of the results obtained in this study with the chromium(III) plating bath combining the acetate and oxalate ions using the Hull cell, with those of other works where chromium(III) plating baths are also prepared. The faradaic efficiency obtained in the bath of this work was 37.5% with the combination of the two additives, being higher than the faradaic efficiency reported with an additive (Table 2).

This faradaic efficiency obtained from 37.5% with a current between 1.6 and 20 A/dm^2 (Fig. 2d) is very good for a chromium coating electrodeposited from Cr(III) bath, since it is very similar to a study reported in Table 2 with high faradaic efficiency and low current[3, 8, 14, 22]. Therefore, the faradaic efficiency obtained with the bath by combining the two additives competes successfully with the faradaic efficiency of the commercial hexavalent baths, which is approximately 12-18%. The experimental faradaic efficiency of the bath of this work is very similar to that reported by Protsenko[2] in a chromium(III) plating bath with other characteristics.

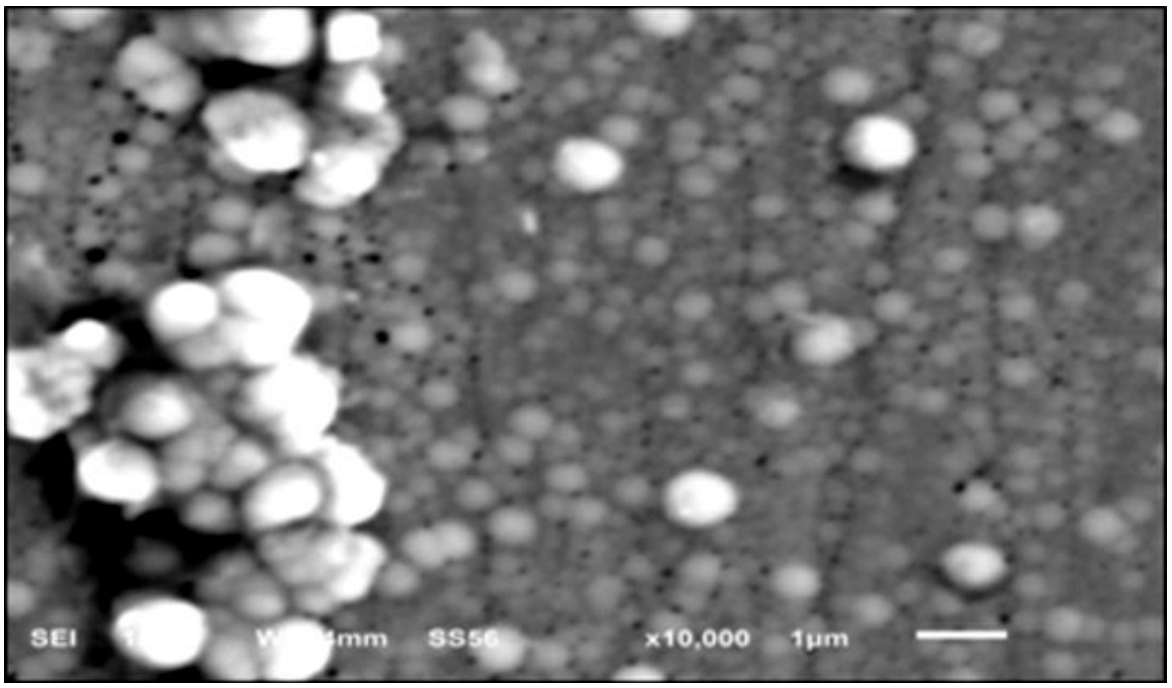

Figure 3. SEM micrograph of the morphology of the 10000x chromium coating where its nodular shape can be seen.

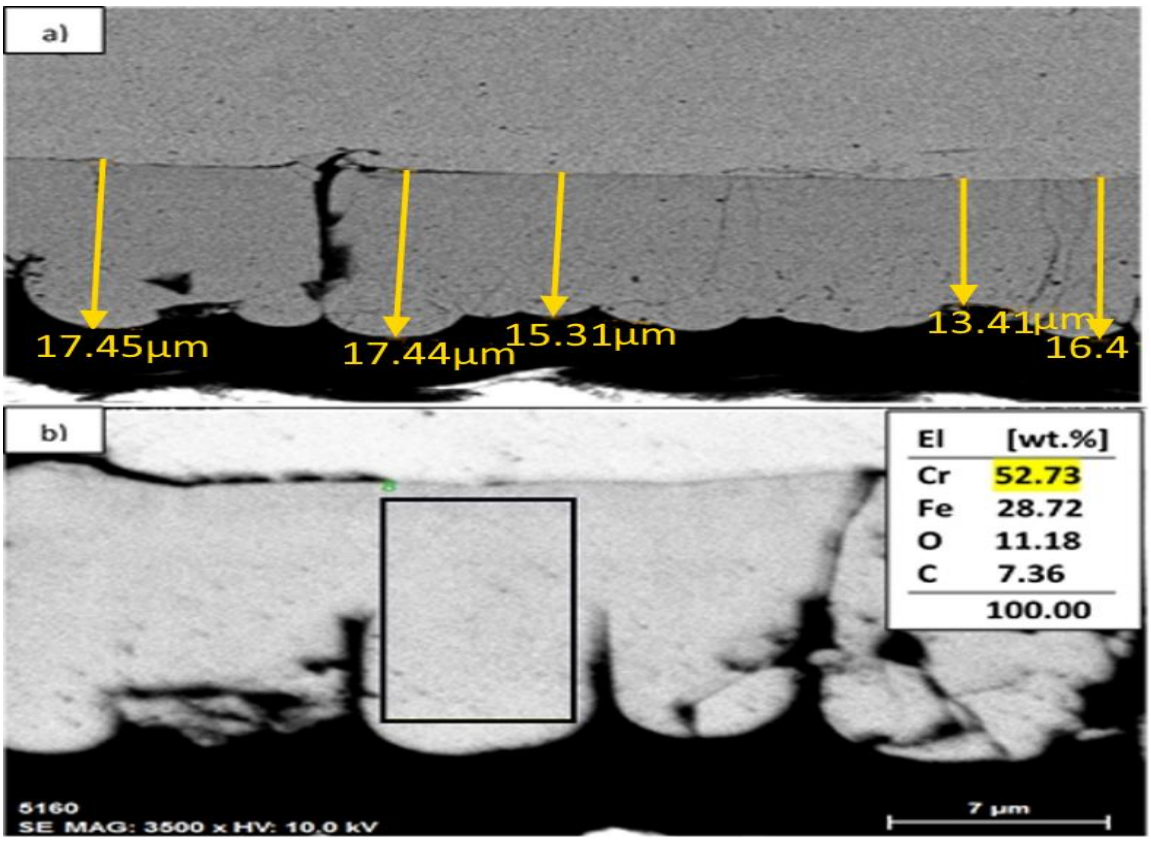

Figure 4. a) Cross-sectional SEM images of the chromium coating obtained from a chromium(III) plating bath with two additives (oxalate and acetate). b) Micrograph of the selected area for EDS of the hard chromium coating obtained from a chromium(III) plating bath with two additives (oxalate and acetate).

In Table 2, the experimental bath deposition rate of this work of 0.4 µm/min is in the range of the reported values (0.4-1.5 µm/min). This important parameter and faradaic efficiency were measured in the Hull cell to evaluate the electrodeposition process. However, Protsenko[2] proposed eighteen parameters for the comparison between chromium(III) and chromium(VI) plating baths, and some of them are shown in Table 2. The temperature and pH in the Cr (VI) and Cr (III) baths are similar, however, the experimental densities of the cathodic current in the Cr (III) baths are lower than the current used in Cr (VI) baths.

Chromium coatings must withstand significant wear, and the hardness of chromium coating electrodeposited from Cr(III) bath depends significantly on grain size, residual stress and inclusions of nonmetallic phases. Hardness measurements were made to the coatings in this work obtained by combining oxalate and acetate ions. The values obtained were 685.7 HV, which is close to the reported value for hard chromium coating (Table 2). Hardness values in the range of 850-950 HV can be observed in chromium(III) plating baths (Table 2)[2, 6, 23-25].

The SEM micrograph (Fig. 3) of the coating shows compact spherical grains with nodular shape characteristic of chromium coating electrodeposited from Cr(III) bath. There are various grain sizes reported in the literature (from 30 µm to 3 nm)[2, 5, 25], and in Fig. 3, the diameters of spherical grains are smaller than 1 µm. Some grains join together and form relatively large nodules, that is, larger than 1

µm. The thickness measurements of the chromium coating electrodeposited from Cr(III) bath were determined by the SEM image of the cross-section for the bath with the combination of the acetate and oxalate ions (Fig. 4a). The thickness was between approximately 14 and 18µm, which is very good since the thickness of the chromium coatings obtained from other reported chromium(III) plating baths is generally 10µm (Table 2).

Table 2. Comparison between studies used Hull Cell.

Bath conditions: principal components, pH, Temperature	**Covering power cm**	**Current density and faradaic efficiency**	**Deposition rate µm/min**	**Thickness (µm)**	**Micro-hardness (HV)**	**References**
Chromium(VI) plating bath, pH 0.1-0.6, 45-55 ^{o}C	6	40-60 A/dm^2 12-18 %	0.2–0.6	300	800-900	[2]
Chromium(III) sulfate 45°C		30 A/dm^2		100	950	[25]
Chromium(III) sulfate (S) Basic chromium(III) sulfate (BS), pH 1.5, 35°C	S 2.4 BS 4.7	S,BS 30-35 A/dm^2 30-35 %	S, BS 0.8-1;1–1.5	S, BS 20	S, BS 800-900	[2]
$CrCl_3.6H_2O$- urea 1:2 eutectic, 40-60 °C		33 A/dm^2 65-74%	0 .416		600	[22]
Formic acid, Basic chromium(III) sulfate (BS)	4.7	A/dm^2	0.7–0.8			[21]
Cr (II): oxalate (1:2), pH 3, 30° C		3 A/dm^2-60 A/dm^2	0.75		No obtained in the hull cell	[17]
Chromium(III) sulfate pH 3.2-3.5, 45-50°C	8.2	30 A/dm^2 37.5 %	0.4	14-18	670	This work

The results of EDS (Fig. 4b) of the chromium coating show that the layer has a high chromium content, which is immediately followed by iron. In addition, small amounts of carbon and oxygen also appeared in the cross-sectional view. Apparently, oxygen and carbon are incorporated into the coating due to the reduction of additives and the DSD in the extremely high electric field[26]. Leimbach[11] postulated that the oxygen observed in the EDS spectrum may be related to the oxidation of the chromium surface in contact with air. Carbon incorporation was also detected by Edigaryan[14] and Safonov[27], and these studies observed the formation of chromium carbide compounds during chromium cathodic deposition from Cr(III) solutions in sulfuric acid in the presence of oxalate ions .

This demonstrates that the combination in the chromium(III) plating bath of the acetate and oxalate ions improves the faradaic efficiency, although the deposited layers contain 7.36% carbon.

Quantitative analysis of carbon in the EDS coating may overestimate the carbon content; that is, it is difficult to separate the carbon signal from that of the sample or from the contaminants accumulated

during the analysis. However, carbon is included in the coating. Li[9] commented that chromium coatings with a higher carbon content have a better hardness, but coatings with less carbon are brighter.

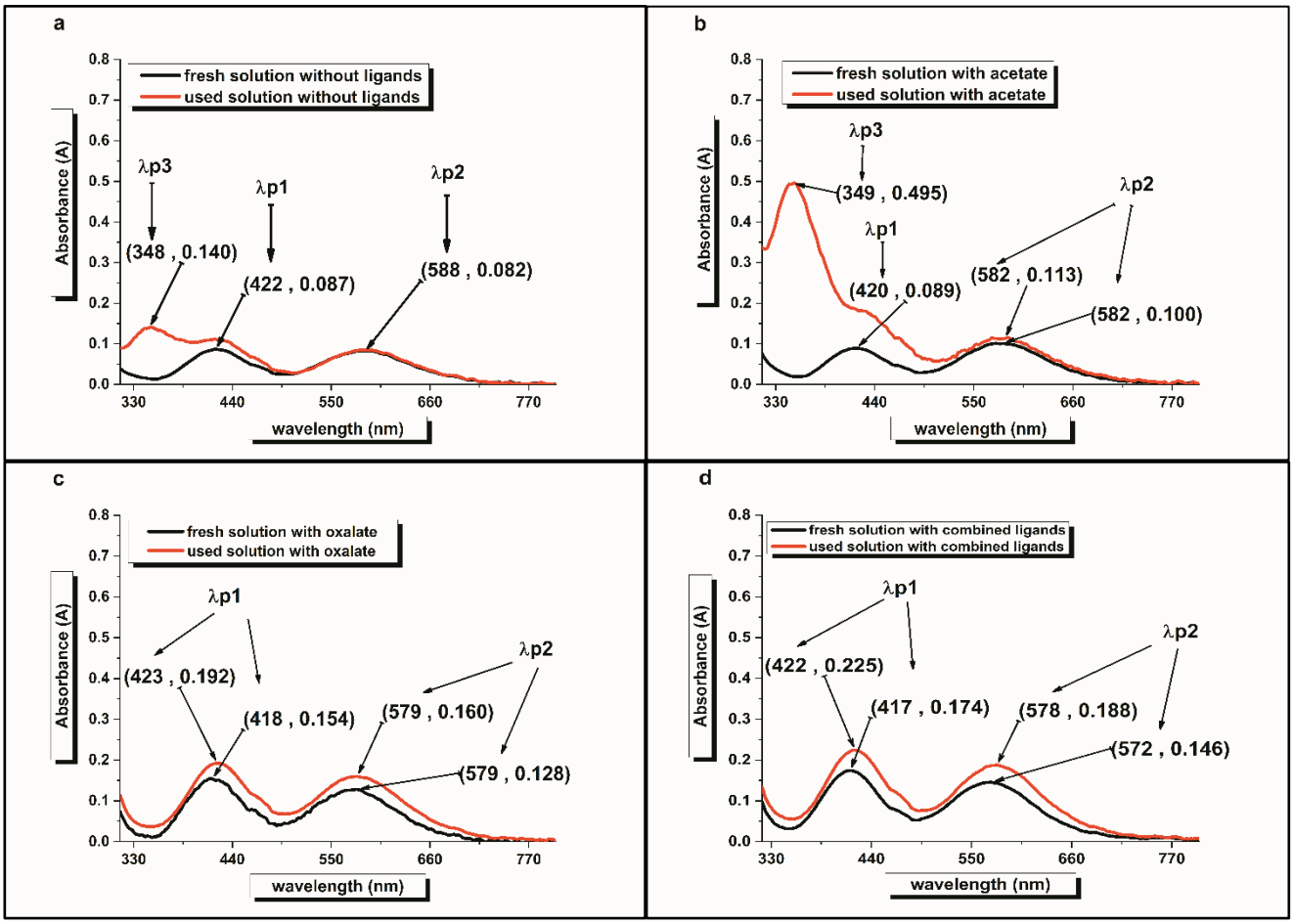

Figure 5. UV–vis absorption spectra. a) bath without additives before (black line) and after electrodeposition (red line); b) bath with acetate additive after electrodeposition (black line) and freshly prepared (red line); c) bath with oxalate additive after electrodeposition (black line) and freshly prepared (red line); d) bath with both additive (acetate and oxalate) freshly prepared (black line) and after electrodeposition (red line). The potential and current between the terminals in the Hull cell were 3A and 7.3V, respectively. The time of electrodeposition was 10 min, and the temperature changed from 23-26°C to 50-55°C.

Recently, Fujishige[28] calculated the excitation energies and orbital characteristics of $[Cr(H_2O)_6]^{3+}$ in an aqueous phase. A transition from the fundamental state to the states of the excited quartet produces two bands at 416.05 nm (2.98 eV) and 587.60 nm (2.11 eV), which are close to the experimental bands observed in the uv-vis absorption spectra of the bath without an additive (black line in figure 5a). Then, the experimental bands at $\lambda1$ = 422 nm and $\lambda2$ = 588 nm indicate that Cr(III) in the fresh chromium bath is mainly in the form of $[Cr(H_2O)_6]^{3+}$ [19, 29]. A change in the values of $\lambda1$ and $\lambda2$ was observed in the bath with the acetate ions (black line in Figure 5b) or oxalate ions (black line in Figure 5c). The main changes in $\lambda1$ and $\lambda2$ were observed when the combination of the two additives (acetate and oxalate ions) was added to the electrodeposition bath (black line in Fig. 5d). The change in

peak height and the change to a slightly shorter wavelength (4 nm-16 nm) are generally interpreted as a ligand exchange reaction[8, 17, 30]. These reactions will be discussed in the next section.

There was a change in the color of the bath after electrolysis in the bath without additive (Fig. 5a); that is, the green of the initial solution changed to a darker green. The bands at λ1 = 422 nm and λ2 = 588 nm remained the same, and a new band appeared in the UV-visible spectrum at 348 nm, which is assigned to $HCrO_4^-$ [31]. Similar results were observed in the acetate ion bath, and the spectrum (Fig. 5b) also revealed that Cr(III) and Cr(VI) were present in the solution. On the other hand, the presence of oxalate ions (Fig. 5c) prevented the formation of Cr(VI). In the presence of the combination of the two additives, the $[Cr(H_2O)_6]^{3+}$ bands (λ1 = 422 nm and λ2 = 588 nm) shifted slightly, and only Cr(III) predominates in the solution. It is not possible to compare the uv-visible spectra after electrolysis with those in the literature because there are no reported spectra of a bath after electrolysis.

Again Protsenko[2] in his work points out that in a Cr(III) bath it will only include traces of Cr(VI), which are formed in a very small amount. In the presence of the oxalate ions we were able to verify that the oxidation of Cr(III) to Cr(VI) is completely avoided.

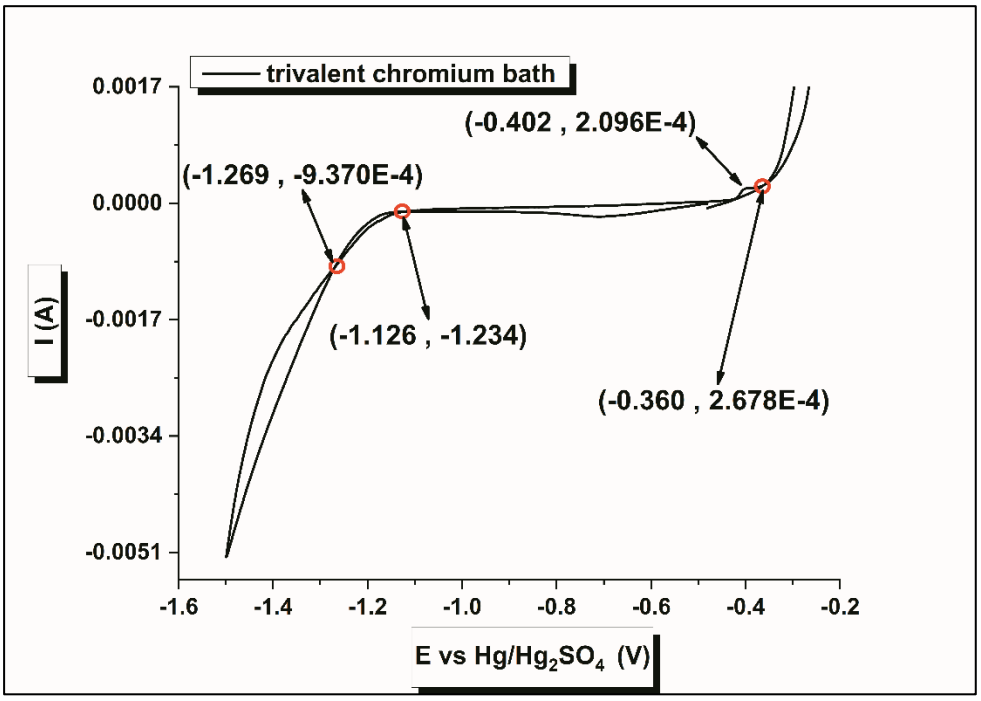

Figure 6. Cyclic voltammetry of the chromium(III) plating bath with the both additives at 5 mV/s, starting with a cathodic potential.

Danilov, Phuong, Abbott, Leimbach and Del Pianta[2, 8, 11, 19, 22] used polarization or voltammetry curves to study the electrodeposition process of chromium from Cr(III) bath. In these studies, it is proposed that the chromium reduction process consists of two partial reactions:

$$Cr^{3+} + e^- \rightarrow Cr^{2+} \quad \textbf{(5)}$$

$$Cr^{2+} + 2e^- \rightarrow Cr^0 \quad \textbf{(6)}$$

In 2010, You[32] reviewed the species presented in the Pourbaix chrome diagram based on IR spectra and XRD patterns. This group proposed that the Cr(III) (aq) and Cr(II) (aq) species predominate at pH values below 3.5. Cr(III) (aq) is a wide-ranging notation of Cr(III) species that does not indicate the particular hydration number of ions, and Fig. 5a presents the complexes defined in the electrodeposition bath. It was difficult to obtain voltammetry curves without very high noise at a more cathodic potential than -0.8 V due to the abundant bubbles that formed from the reaction (7).

$$2H_3O^+ + 2e^- \rightarrow H_2\uparrow + 2H_2O \qquad \textbf{(7)}$$

In Fig. 6, the initial potential is approximately -0.49 V, will be in the double layer region, and the current will be lower when it is swept in the cathodic direction. When the potential reaches at least -0.49 V, the current decreases due to reactions (5-7). When scanning is performed in the anodic direction, two crosses are observed between the anodic and cathodic curves at -0.559 V and -0.416 V, which are characteristic of electrodeposition systems. At positive potentials, the oxidation peak at 0.35 V was caused by oxidation of the substrate metal (brass).

Figure 6 also shows that the hydrogen evolution reaction (7) (E_0 = 0.0 V) requires a high overpower in the bath. In addition, reaction (6) also requires a high overpotential because the thermodynamic potential of reaction (5) is -0.0615 V, which was calculated using the Nernst equation (8). The thermodynamic potential of the reaction (6) is -0.0853 V, see equation (9), this potential did not allow voltammetry measurements due to the formation of bubbles. The voltamogram in Fig. 6 also shows that the reduction of Cr(III) in aqueous solution is kinetically slow, so that the overpotential for electrodeposition is very high. Therefore, the hydrogen evolution reaction is the dominant reaction in the cathode.

In aqueous media, the predominance diagram shows the formation of the species $[Cr(H_2O)_6]^{3+}$ at a pH value of 3.5 (Fig.7a), and in the presence of sulfate ions, the predominant complex in the bath of electrodeposition is $Cr_2(SO_4)_3$ (Fig.7b). Del Pianta[19] observed two reduction peaks in the voltamograms of $Cr_2(SO_4)_3$ solutions at a pH value of 3.5. This result suggests that the reduction of Cr(III) is carried out in a two-step process through the formation of Cr(II). The voltammetry results in Fig. 6 provide evidence of a two-step process and indicate the possibility that the reduction of Cr(III) to Cr(0) occurs in a single step in the presence of oxalate and acetate ions.

$$E_t = E_t^o + \frac{2.303RT}{F}\log\frac{a_{Cr^{3+}}}{a_{Cr^{2+}}} = -0.378V + 0.0578V * \log\frac{0.3}{(0.3\text{-}10^{-6})} = -0.06156V \qquad \textbf{(8)}$$

$$E_t = E_t^o + \frac{2.303RT}{2F}\log a_{Cr^{2+}} = -0.838V + (0.0578/2V) * \log 0.3 = -0.0853V \qquad \textbf{(9)}$$

Perelygin[33] calculated the concentrations of boric acid and its ionic species in the range of pH 0-14 with the conclusion that H_3BO_3 predominates at pH 3.5. Boric acid is a substance that donates protons and acts satisfactorily as a pH buffer; for example, after 2h of the electrodeposition process, the pH values varied only 0.2 units. In the 300 ml working cell, a water loss of approximately 15% was

observed after 2h of electrolysis. The hydrogen gas bubbles generated during the process carried water vapor with them, and the formation of hydrogen gas (7) transforms approximately 6 ml of water into hydrogen gas according to the faradaic efficiency.

It is known that boric acid is a Lewis acid because it accepts the solitary pair of electrons from water oxygen. Then, the boric compound is converted into a boric water complex that is similar to a protonated species, and from this compound, a proton is donated. Consequently, the boric compound also behaves like a Bronsted acid. This explains the minimum changes in the pH values observed during 2h of electrolysis. It is important to keep in mind that at the pH values studied, several water molecules are constantly associated with borate molecules.

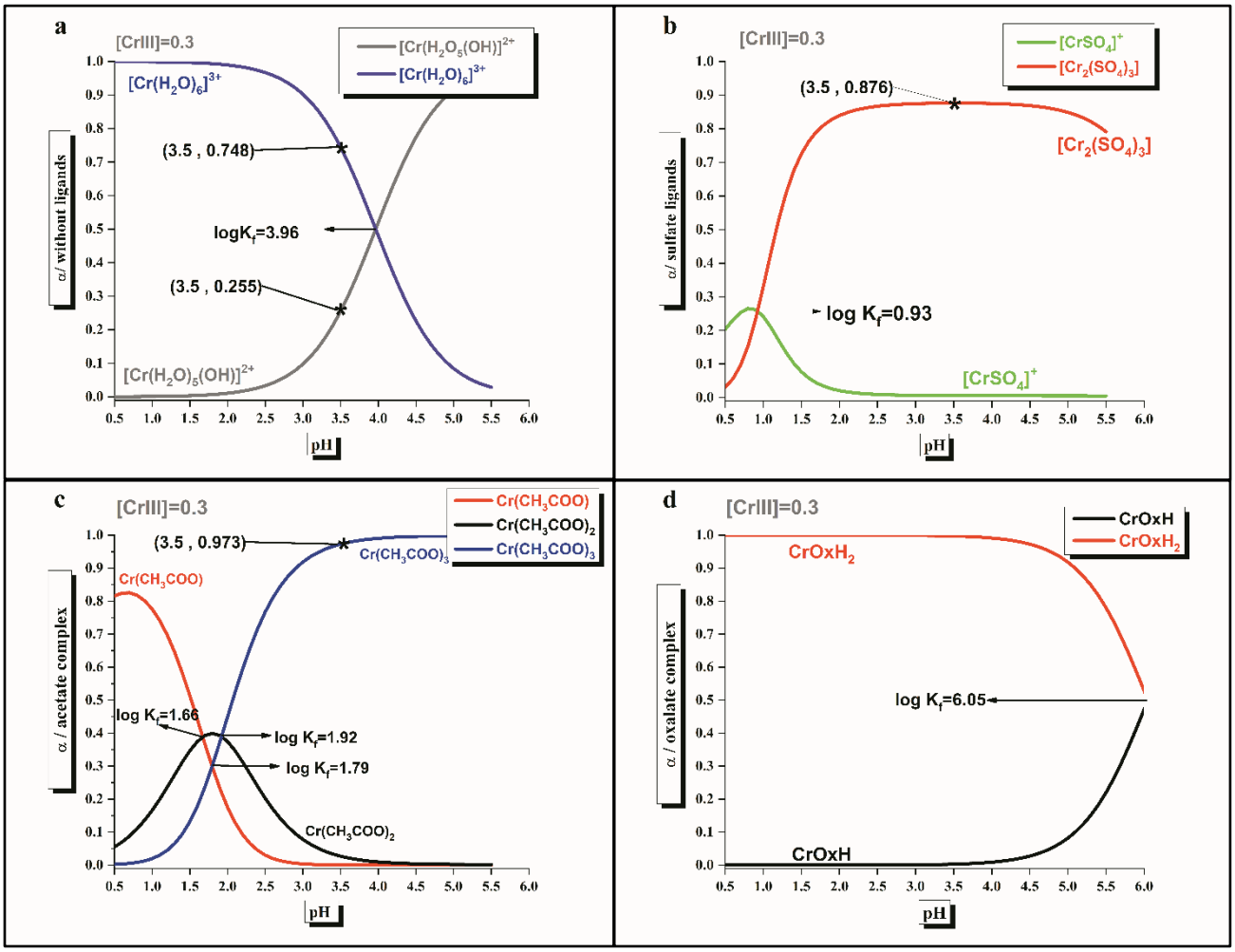

Figure 7. Predominance diagrams. a) aqueous media, b) aqueous media with sulfate anions, c) aqueous media with acetate anions, d) aqueous media with oxalate anions.

Sodium dodecyl sulfate (SDS) is generally the surfactant that is included in chromium(III) plating baths [2, 4, 6, 7, 11, 23, 34-38]. Although it is not expected to reach the critical micellar concentration, hydrophobic interactions of the chains of sodium dodecyl sulfate molecules tend to form the nucleus of a micelle, while polar head groups are in the immediate vicinity of the ions of solvation

Figure 8 will provide a schematic representation of the isolated volumes of a chromium(III) plating bath with a rigid structure caused by electrostatic attractions and repulsions[39] . The main group of SDS is anionic, and the sodium counterion can be easily replaced by the solvated Cr(III) ion. This small volume contains a limited number of Cr(III) ions and, consequently, a small grain size will be obtained in the electrodeposition process.

Danilov[23] reported that the hardness value increases when SDS is added to the coating bath, which implies small grain sizes. In addition, the proposed orientations of the acetate and oxalate ions in these small aggregates are included in Fig. 8. This structure of the isolated solvated Cr(III) ions obstructs the formation of polymeric oxides (olation reactions) by minimizing the number of Cr(III) ions nearby. The electrostatic repulsion between two ions $[Cr(H_2O)_6]^{3+}$ is extremely strong, and will lead to the inevitable formation of dimers in the bath; however, this repulsion will decrease as complex charges are reduced by deprotonation (11), which will facilitate the approach and contact between the species that react in the reaction (10).

$$[Cr(H_2O)_5OH]^{2+}+[Cr(H_2O)_6]^{3+} \rightarrow \text{dimer} \qquad k_{1.0}=6.\ 10^{-6} \qquad \textbf{(10)}$$

$$[Cr(H_2O)_6]^{3+} \leftrightarrow \quad [Cr(H_2O)_5(OH)]^{2+} + H^{+} \qquad \textbf{(11)}$$

The high buffer capacity of boric acid and the small volumes produced by SDS make reactions (10) and (11) difficult, but these reactions will still occur. Therefore, the combination of acetate and oxalate ions will be added to the bath to completely suppress these reactions.

Most previous studies[40, 41] assume that acetate[4], formiate[13, 42] and oxalate[14] can play the role of ligands, L^n, in $Cr^{3+}(H_2O)_mL^{n+}$, and in consequently, a ligand exchange reaction between the additives and Cr(III) has been proposed, which involves the replacement of water molecules with an acetate or oxalate anion in the internal coordination sphere. For example, in the presence of aminoacetic acid, Danilov[43] proposed that five coordination sites in the internal coordination sphere of a complex are occupied by water molecules and one by L. The formation of the proposed complex is based on spectroscopy and mass uv-visible balances obtained by electrochemical or chromatographic methods.

There is no evidence of the chemical nature of the complex Cr(III) by methods that directly determine the molecular structure, for example, nuclear magnetic resonance spectroscopy, vibrational spectroscopy, wide-angle X-ray scattering, etc. Therefore, in the chromium(III) plating bath described in Table I, the formation of complexes by ligand exchange reaction must be carefully considered because the d-orbitals of $[Cr(H_2O)_6]^{3+}$ are completely filled with electrons; therefore, it is not possible for a ligand to replace a water molecule. It is likely that the interactions of the water molecules coordinated with Cr(III) and with the additives placed in the second solvation sphere will facilitate the reduction of active Cr(III) species.

Jackson[44, 45] using nuclear magnetic resonance spectroscopy ^{17}O demonstrates that hexaaquo hydration of Al(III) and Cr(III) is stable because the exchange of solvent water in the hydration sphere is extremely slow. Water molecules in $[Cr(H_2O)_6]^{3+}$ exchange from the inner sphere to the second sphere every ~380 months (half-life ~10^9 s)[46] . Putting this into perspective, although Cr(III) and Ga(III) have

very similar M-O link distances in the first hydration sphere, Cr(III) exchanges 10^{-9} times slower than Ga(III) [47]. It has been established that the first hydration sphere of water molecules forms strong ~12 hydrogen bonds to the second sphere[48, 49], and the lifespan of hydrogen bonds between water molecules of the second and third sphere is of the order of 128×10^{-12} s [50]. There are 20 hydrogen bonds in the third hydration sphere (~10 water molecules). We propose that the protonated species of the acetate and oxalate ions will form hydrogen bonds with the waters in the first or second Cr(III) hydration spheres; that is, Cr(III) interacts so strongly with the water molecules in the first hydration sphere that even the water molecules or ions of the second sphere are relatively tightly bound[50].

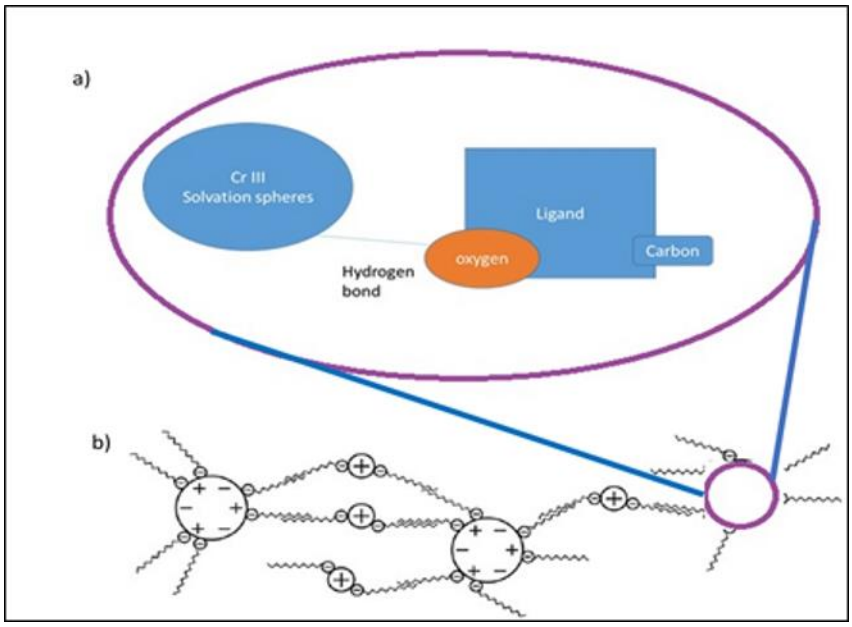

Figure 8. Idealized scheme of the structure proposed by the formation of small volumes; in the magnified inset the possible orientations of the acetate and oxalate ions between the aquo-complex and SDS are considered.

In a very simplified image of determining the coordination number of water molecules with ions, there are 2.43 M of ions (Table 1) and 56.6 M of water in the coating bath with all the compounds; therefore, there are 23 water molecules per ion. Some of them are strongly attached; for example, Na^+ has 5.6 water molecules in the first solvation sphere[51] and most likely 10 in the second sphere; consequently, only 8 can form the mass phase and the third solvation sphere. The species are so close together that a strong electric force is generated between them. On the other hand, at pH 3.5, there is competition between Cr(III) ions and acetate and oxalate ions for protons. As mentioned earlier, an explanation that coincides with these problems is the formation of hydrogen bonds between the water molecules in the first Cr(III) solvation sphere and the acetate or oxalate ions in the second sphere.

The dielectric constant measures the ability of a substance to maintain charge separation, and a solvent must have a sufficiently high dielectric constant (σ) to ensure the dissociation of $Cr_2(SO_4)_3$ dissolved to separate ions. The H_2O (σ 80) and HSO_4^- (σ 84) molecules have higher dielectric constants than boric acid (σ 5), acetic acid (σ 4.1) and oxalic acid (σ 3). Consequently, the $[Cr(H_2O)_6]^{3+}$ (Fig. 7a) and $[Cr_2(SO_4)_3]$ (Fig. 7b) complexes are only feasible, while the acetic (Fig. 7c) and oxalic (Fig. 7d)

should be interpreted as $Cr^{3+}(H_2O)_mL^{n+}$, where L is in the second solvation sphere. The introduction of ions into the second solvation sphere can result in electrostatic deformation in the water molecules of the first sphere in a direction against the electrostatic attraction of Cr(III). At that point, the water molecules in the first solvation sphere are subject to two opposite electrostatic forces at their ends and, consequently, the Cr(III) oxygen bond distance in the first sphere (1.966 Å) could increase. This explanation is based on the high stabilization energy of Cr-O bonds in $[Cr(H_2O)_6]^{3+}$, which are more than 40 kJ/mol stronger than a "normal" M-O bond[30]. Then, in Fig. 7c and 7d, the ligand L^n of the $Cr^{3+}(H_2O)_mL^{n+}$ complex is most likely located in the second solvation sphere, and these compounds have different wavelengths and absorbance (see Fig. 5).

Oxalate dissolves in the aqueous mass, and the number of water molecules in the first solvation sphere is approximately 15[52]. However, in the bath, there are not enough water molecules to form a second solvation sphere. Consequently, we propose that Cr(III) and oxalate ions can share their solvation water. In contrast, Zeng[17] proposed a ligand exchange reaction in which an oxalate molecule replaced a water molecule in the first solvation sphere of $[Cr(H_2O)_6]^{3+}$ and formed $[Cr(H_2O)_5OOCCOOH]^{2+}$. However, this process has a steric hindrance because the molar volume of oxalate (55 cm^3mol^{-1})[53] is three times greater than the molar volume of water (17.969 cm^3mol^{-1})[53]. On the other hand, Protsenko[15] proposed reaction 12, and in our study, it is suggested that the number n of water is 6 and that oxalate ions are in the second sphere of solvation.

$$[Cr^{2+}(C_2O_4)(H_2O)_n]_{ads} + 2H^+ + 2e^- \rightarrow Cr^0 + H_2C_2O_4 + nH_2O \quad \textbf{(12)}$$

4. CONCLUSIONS

The Hull cell was used effectively to determine the optimal composition of the bath, as shown in Table 1. The bath with the combination of acetate and oxalate ions had a very good faradaic efficiency (37%), high covering power (8.2 cm), low deposition potential (7.3 V) and good deposition rate (0.4μm/min). Although electrodeposition was performed at a current density (30 A/dm^2), the state of the art briefly summarized (Tables 2) leads to the conclusion that this chromium(III) plating bath is competitive for the chrome plating industry.

For deposits obtained in cells with parallel plates, the thickness was approximately 10 μm, and the hardness was 685.7 HV. The deposit has spherical grains with diameters less than 1 μm, and some grains join to form larger nodules. The content of Cr(VI) in the bath after electrodeposition with the combined ions was undetectable, the residual water will be essentially free of Cr(VI), which implies a lower cost in the treatment of residuals.

Voltamograms are difficult to analyze in a bath with several elements. However, the results obtained indicate that the reduction of Cr(III) to Cr(0) occurs in one step in the presence of the combination of oxalate and acetate ions (reaction 11). Sodium dodecyl sulfate molecules tend to form the nucleus of a micelle, which results in small volumes that can influence grain size. These small volumes and the buffer capacity of boric acid impose a barrier to olation reactions; These reactions can be completely avoided as demonstrated in this bath when a combination of the acetate and oxalate ions

was added. In the literature, bidentate ligands, such as oxalate anions, have been reported to replace water molecules in the inner sphere of $[Cr(H_2O)_6]^{3+}$. Then, a ligand exchange reaction forms a complex such as $[Cr(H_2O)_5OOCCOOH]^{2+}$, and this proposition is based on results of uv-visible spectroscopy. At this point, an alternative approach is presented in our work to explain the structure of the compound $Cr(H_2O)_6H_2C_2O_4$.

This new proposal is based on the high stability of the first Cr(III) solvation sphere and the influence of this metal on the second solvation sphere, where the combined oxalate and acetate ions are likely to be found. Therefore, the water molecules in the first solvation sphere are going to be exposed to two opposite electrostatic forces at their ends, and consequently, the distance of the Cr(III) oxygen bond with the water molecules in the first solvation sphere can increase. This link elongation process is what facilitates the electroreduction of these active species of trivalent chromium.

ACKNOWLEDGMENTS
The authors thank the Mexican Council of Science and Technology (CONACYT) for the financial support for carrying out this work. D. Fernández also thanks CONACYT for a postgraduate scholarship.

References

1. C. Kasper, *B.S. Jour. Research*, 11 (1933) 515.
2. V. S. Protsenko, F. I. Danilov, *Clean Techn Environ Policy*, 16 (2014) 1201.
3. I. Drela, J. Szynkarczuk, J. Kubicki, *J. Appl. Electrochem.*, 19 (1989) 933.
4. Y. B. Song, D.-T. Chin, *Electrochim. Acta*, 48 (2002) 349.
5. G. Saravanan, S. Mohan, *J. Appl. Electrochem.*, 40 (2010) 1.
6. V. S. Protsenko, F. I. Danilov, V. O. Gordiienko, S. C. Kwon, M. Kim, J. Y. Lee, *Thin Solid Films*, 520 (2011) 380.
7. V. S. Protsenko, V. O. Gordiienko, F. I. Danilov, S. C. Kwon, M. Kim, J. Y. Lee, *Surf. Eng.*, 27 (2011) 690.
8. N. V. Phuong, S. C. Kwon, J. Y. Lee, J. H. Lee, K. H. Lee, *Surf. Coating. Technol.*, 206 (2012) 4349.
9. L. Li, Z. Wang, M.-y. Wang, Y. Zhang, *Int. J. Miner. Metall. Mater.*, 20 (2013) 902.
10. J. H. O. J. Wijenberg, M. Steegh, M. P. Aarnts, K. R. Lammers, J. M. C. Mol, *Electrochim. Acta*, 173 (2015) 819.
11. M. Leimbach, C. Tschaar, U. Schmidt, A. Bund, *Electrochim. Acta*, 270 (2018) 104.
12. H. T. S. Britton, O. B. Westcott, *Trans. Far. Soc.*, 28 (1932) 627.
13. F. I. Danilov, V. S. Protsenko, T. E. Butyrina, *Russ. J. Electrochem.*, 37 (2001) 704.
14. A. A. Edigaryan, V. A. Safonov, E. N. Lubnin, L. N. Vykhodtseva, G. E. Chusova, Y. M. Polukarov, *Electrochim. Acta*, 47 (2002) 2775.
15. V. Protsenko, F. Danilov, *Electrochim. Acta*, 54 (2009) 5666.
16. Z. Zeng, Y. Sun, J. Zhang, *Electrochem. Commun.*, 11 (2009) 331.
17. Z. Zeng, Y. Zhang, W. Zhao, J. Zhang, *Surf. Coating. Technol.*, 205 (2011) 4771.
18. N. A. Polyakov, *Russ. J. Electrochem.*, 52 (2016) 858.
19. D. D. Pianta, J. Frayret, C. Gleyzes, C. Cugnet, J. C. Dupin, I. L. Hecho, *Electrochim. Acta*, 284 (2018) 234.
20. M. J. L. Gines, F. J. Williams, C. A. Schuh, *J. Appl. Surf. Fin.*, 2 (2007) 112.
21. F. I. Danilov, V. S. Protsenko, V. O. Gordiienko, A. S. Baskevich, V. V. Artemchuk, *Prot. Met. Phys. Chem. Surf.*, 49 (2013) 299.

22. A. P. Abbott, A. A. Al-Barzinjy, P. D. Abbott, G. Frisch, R. C. Harris, J. Hartley, K. S. Ryder, *Phys.Chem.Chem.Phys.*, 16 (2014) 9047.
23. F. I. Danilov, V. S. Protsenko, V. O. Gordiienko, S. C. Kwon, J. Y. Lee, M. Kim, *Appl. Surf. Sci.*, 257 (2011) 8048.
24. V. S. Protsenko, F. I. Danilov, V. O. Gordiienko, A. S. Baskevich, V. V. Artemchuk, *Int. J. Ref. Met. Har. Mat.*, 31 (2012) 281.
25. J. Li, Y. Li, X. Tian, L. Zou, X. Zhao, S. Wang, S. Wang, *Mater. Sci. Appl.*, 08 (2017) 1014.
26. V. S. Protsenko, V. O. Gordiienko, F. I. Danilov, *Electrochem. Commun.*, 17 (2012) 85.
27. V. A. Safonov, L. N. Vykhodtseva, Y. M. Polukarov, O. V. Safonova, G. Smolentsev, M. Sikora, S. G. Eeckhout, P. Glatzel, *J. Phys. Chem. B*, 110 (2006) 23192.
28. S. Fujishige, Y. Kawashima, N. Yoshida, H. Nakano, *J. Phys. Chem. A*, 117 (2013) 8314.
29. D. A. Johnson, *J. Electrochem. Soc.: Electrochemical Science and Technology*, 132 (1985) 1058.
30. B. C. Bunker, W. H. Casey, in *The Aqueous Chemistry of Oxides*, Oxford University Press 2016, Chap. 4, pp. 62-86.
31. P. R. Patrício, R. C. Cunha, S. J. R. Vargas, Y. L. Coelho, L. H. M. d. Silva, M. C. H. d. Silva, *Sep. Purif. Technol.*, 158 (2016) 144.
32. Y. Hai-xia, X. Hong-bin, Z. Yi, Z. Shi-li, G. Yi-ying, *Trans. Nonferrous Met. Soc. China*, 20 (2010) s26.
33. Y. P. Perelygin, D. Y. Chistyakov, *Russ. J. Appl. Electrochem.*, 79 (2006) 2041.
34. J. Kotas, Z. Stasicka, *Environ. Pollut.*, 107 (2000) 263.
35. S. Ghaziof, M. A. Golozar, K. Raeissi, *J. Alloys Compd.*, 496 (2010) 164.
36. V. S. Protsenko, V. O. Gordiienko, F. I. Danilov, S. C. Kwon, *E-J. Chem.*, 8 (2011) 1925.
37. M. Rezaei-Sameti, S. Nadali, J. Rajabi, M. Rakhshi, *J. Mol. Structure*, 1020 (2012) 23.
38. W. Wang, H. Bai, H. Li, Q. Lv, Z. Wang, Q. Zhang, *J. Electroanal. Chem.*, 794 (2017) 148.
39. G. D. Falco, A. Porta, A. M. Petrone, P. D. Gaudio, A. E. Hassanin, M. Commodo, P. Minutolo, A. Squillace, A. D'Anna, *Environ. Sci.: Nano*, 4 (2017,) 1095.
40. E. G. Vinokurov, V. V. Bondar, *Koord. Khim*, 29 (2003) 66.
41. E. G. Vinokurov, A. V. Demidov, V. V. Bondar, *Koord. Khim*, 30 (2004) 774.
42. C.-E. Lu, N.-W. Pu, K.-H. Hou, C.-C. Tseng, M.-D. Ger, *Appl. Surf. Sci.*, 282 (2013) 544.
43. F. I. Danilov, V. S. Protsenko, *Zashch. Met.*, 37 (2001) 223.
44. J. A. Jackson, J. F. Lemons, H. Taube, *J. Chem. Phys.*, 32 (1960) 553.
45. M. A. Jr., J. A. Jackson, *J. Chem. Phys.*, 41 (1964) 3402.
46. L. Helm, A. E. Merbach, *Chem. Rev.*, 105 (2005) 1923.
47. P. Lindqvist-Reis, A. Muñoz-Páez, S. Díaz-Moreno, S. Pattanaik, I. Persson, M. Sandstrom, *Inorg. Chem.*, 37 (1998) 6675.
48. P.-A. Bergstrom, J. Lindgren, M. Read, M. Sandstrom, *J. Phys. Chem.*, 95 (1991) 7650.
49. A. Mufioz-Paez, E. S. Marcos, *J. Am. Chem. Soc.*, 114 (1992) 6931.
50. A. Cusanelli, U. Frey, D. T. Richens, A. E. Merbach, *J. Am. Chem. Soc.*, 118 (1996) 5265.
51. C. Liu, F. Min, L. Liu, J. Chen, *Chem. Phys. Lett.*, 727 (2019) 31.
52. O. Kroutil, B. Minofar, M. Kabeláč, *J. Mol. Model.*, 22 (2016) 210.
53. C. L. Yaws, *Yaws' Critical Property Data for Chemical Engineers and Chemists*. Knovel, 2012 2014